Solution Structure of *Eucommia* Antifungal Peptide: A Novel Structural Model Distinct with a Five-Disulfide Motif[†,‡]

Ren-Huai Huang,[§] Ye Xiang,[§] Guan-Zhong Tu,[#] Ying Zhang,[§] and Da-Cheng Wang*[,§]

Center for Structural and Molecular Biology, Institute of Biophysics, Chinese Academy of Sciences, Beijing 100101, and Beijing Institute of Microchemistry, Beijing 100087, P. R. China

Received December 17, 2003; Revised Manuscript Received March 12, 2004

ABSTRACT: The three-dimensional structure in aqueous solution of *Eucommia* antifungal peptide 2 (EAFP2) from *Eucommia ulmoides* Oliv was determined using ^{1}H NMR spectroscopy. EAFP2 is a newly discovered 41-residue peptide distinct with a five-disulfide cross-linked motif. This peptide exhibits chitin-binding activity and inhibitory effects on the growth of cell wall chitin-containing fungi and chitin-free fungi. The structure was calculated by using torsion angle dynamic simulated annealing with a total of 614 distance restraints and 16 dihedral restraints derived from NOESY and DQF-COSY spectra, respectively. The five disulfide bonds were assigned from preliminary structures using a statistical analysis of intercystinyl distances. The solution structure of EAFP2 is presented as an ensemble of 20 conformers with a backbone RMS deviation of 0.65 (±0.13) Å for the well-defined Cys3−Cys39 segment. The tertiary structure of EAFP2 represents the first five-disulfide cross-linked structural model of the plant antifungal peptide. EAFP2 adopts a compact global fold composed of a 3_{10} helix (Cys3−Arg6), an α-helix (Gly26−Cys30), and a three-strand antiparallel β-sheet (Cys16−Ser18, Tyr22−Gly24, and Arg36−Cys37). The tertiary structure of EAFP2 shows a chitin-binding domain (residues 11−30) with a hydrophobic face and a characteristic sector formed by the N-terminal 10 residues and the C-terminal segment cross-linked through the unique disulfide bond Cys7−Cys37, which brings all four positively charged residues (Arg6, Arg9, Arg36, and Arg40) onto a cationic face. On the basis of such a structural feature, the possible structural basis for the functional properties of EAFP2 is discussed.

During the last two decades, over 500 antimicrobial peptides have been discovered from animals and plants (see review in ref *1*). The antimicrobial peptides are found so diverse that it is difficult to categorize them except broadly on the basis of their secondary structure and the disulfide-pairing pattern (*1*, *2*). The disulfide-rich peptides formed a large group. The plant antimicrobial peptides all have a compact structural motif stabilized by disulfide bonds arranged in a distinct pairing pattern (*2*, *3*). Accordingly, the plant antimicrobial peptides are usually classified as plant defensins, thionins, hevein-like, and knottin-like peptides, etc. (*2*, *3*) by their distinct disulfide patterns and sequence similarities.

Among them, the hevein-like peptides, such as hevein from laticifers of rubber tree (*4*, *5*), antimicrobial peptides from *Amaranthus caudatus* seeds (Ac-AMP) (*6*, *7*), and antifungal peptides from the seeds of *Pharbitis nil* (Pn-AMP) (*8*), have specific chitin-binding activities and are characterized by three or four disulfides to stabilize a chitin-binding domain referred as hevein domain (*2*, *9*) as shown in Figure 1. This hevein domain mostly consists of 30−43 residues including six or eight cysteines pairing into three or four disulfide bonds, three aromatic residues, two glycines, and one serine (Figure 1) and occurs in a variety of plant proteins and peptides in multiple or single copies, respectively (*2*). Their antifungal activities are assumed to be associated with their potential chitin-binding activities since chitin is the main structural component of the fungal cell wall (*9*, *10*).

The *Eucommia* antifungal peptide 2 (EAFP2)[1] is a newly discovered 41-residue peptide with pyroglutamic blockage at the N-terminus, which is purified from the bark of *Eucommia ulmiodes* Oliv (*11*−*13*) (Figure 1). It has 34, 39, and 51% sequence identities with hevein (*4*), Ac-AMP (*6*), and Pn-AMP (*8*), respectively. However, EAFP2 contains 10 cysteines, which are cross-linked to form five disulfide bridges (*11*). This is the first finding of a plant antifungal peptide with a five-disulfide motif, which represents a novel type of antifungal peptide (*11*). The antimicrobial assay shows that EAFP2 exhibits relatively broad spectrum of antifungal activities against eight tested agricultural pathogenic fungi from cotton, wheat, potato, tomato, and tobacco

[†] This work was supported by the MOST (863-2002BA711A13; G19990756), NNSF (30070162) of China, and CAS (KSCX1-WS-17).

[‡] The table of ^{1}H chemical shifts has been deposited in the BioMagResBank under accession code BMRB-5795. The atomic coordinates for the ensemble of 20 conformers have been deposited in the RCSB Protein Data Bank under accession code 1P9Z.

* Corresponding author: Da-Cheng Wang, Center for Structural and Molecular Biology, Institute of Biophysics, Chinese Academy of Sciences, 15 Datun Road, Beijing 100101, PR. China. Tel: (86)-10-64888547; fax: (86)-10-6488 8560; e-mail: dcwang@sun5.ibp.ac.cn.

[§] Chinese Academy of Sciences.

[#] Beijing Institute of Microchemistry.

[1] Abbreviations: EAFP2, *Eucommia* antifungal peptide 2 from the bark of *Eucommia ulmoides* Oliv; NMR, nuclear magnetic resonance; COSY, correlated spectroscopy; DQF-COSY, double-quantum-filterer correlated spectroscopy; NOE, nuclear Overhauser effect; NOSEY, nuclear Overhauser effect spectroscopy; TOCSY, total correlation spectroscopy; RMS, root-mean-square; 1D, one dimensional; 2D, two dimensional.

10.1021/bi036263y CCC: $27.50 © 2004 American Chemical Society
Published on Web 04/27/2004

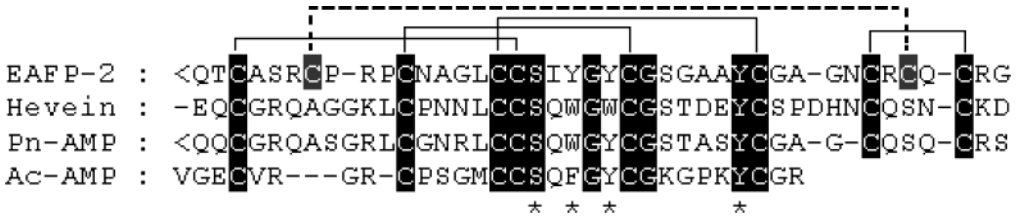

FIGURE 1: Sequence of EAFP2 (*11*) in alignment with Hevein (*4*), Pn-AMP (*8*), and Ac-AMP (*6*). The identical residues are shadowed in black and the additional two cysteines of EAFP2 are in gray. The four asterisks at the bottom indicate the residues critical for chitin binding. The full lines at the top show connectivities of cysteines in hevein and the dotted line shows the unique disulfide bridge in EAFP2.

(*11*). Interestingly, they can inhibit the growths of not only the chitin-containing fungi, but also the chitin-free fungi (*11*). This indicates that chitin-binding affinity is not essential for EAFP2 to exert an inhibitory action on fungal growth. In addition, EAFP2 can retain its activity in boiling water for 30 min, and 5 mmol/L calcium ion can decrease its inhibitory effect by more than 20 times (*11*). To further understand the structure−function relationship of this novel antifungal peptide, the three-dimensional structure is required.

In this paper, the solution structure of EAFP2 determined by using two-dimensional ^{1}H NMR spectroscopy and ab initio torsion angle dynamic simulated annealing (*14*) is reported. The structure analysis showed that EAFP2 adopts a compact global fold composed of a 3_{10} helix (Cys3−Arg6), an α-helix (Gly26−Cys30), and a three-strand antiparallel β-sheet (Cys16−Ser18, Tyr22−Gly24, and Arg36−Cys37). The significant feature of the EAFP2 tertiary structure compared with the chitin-binding peptide and the role of the fifth disulfide bridge distinct from the hevein domain in the tertiary structural arrangement will be described. Furthermore, the antifungal mechanisms of EAFP2 will also be discussed.

MATERIALS AND METHODS

Sample Preparation. EAFP2 was purified from the bark of *E. ulmoides* Oliv as described previously (*11*). The peptide purity was confirmed by reverse phase HPLC and MALDI-TOF mass spectrometry. The NMR sample was prepared by dissolving 12 mg of lyophilized EAFP2 in 500 μL of 20 mmol/L sodium phosphate buffer (pH 5.6) containing 10 μmol/L EDTA, 0.002% NaN_3, and 10% ^2H_2O. For experiments in ^2H_2O, the above sample was repeatedly lyophilized and dissolved in 99.8% ^2H_2O, and the final sample was dissolved in 99.996% ^2H_2O. Sodium 3-(trimethyl-silyl) propionate-2,2,3,3-D4 (TSP) was added as the internal chemical shift reference with the final concentration of 0.2 mmol/L.

NMR Measurements. The proton NMR spectra including DQF-COSY, TOCSY, and NOESY were collected on a Bruker DMX 500 spectrometer equipped with the Cryoprobe (Bruker, Rheinstetten, Germany) in a phase-sensitive mode by the time-proportional phase incrementation (TPPI) method following standard pulse sequences and phase cycling. Solvent suppression was achieved by the presaturation method. Typically, the 2D ^{1}H NMR experiments were performed with acquisition of 256 or 512 t_1 increments, 16 scans per increment and 2048 or 4096 data points per scan. The NMR data were processed using Xwinnmr (Bruker) and analyzed using Sparky (*15*). Before Fourier transformation, the sine bell or sine bell square window functions were applied with phase shift of $\pi/2$ or $3\pi/2$.

The Disulfide Assignment. The disulfide-pairing pattern is obtained by using a statistical analysis (*16*) of intercystinyl distances from preliminary structures. Initially, a series of three-dimensional structures was calculated by CNS solve (*17*) with restraints of dihedral angles and NOE distances without any assumptions about disulfide bonds. From 50 computed structures, 12 conformers were selected, in which the angle violations are less than 2 degrees, distance violations less than 0.2 angstroms, and the total energy of each conformer less than 20 kcal mol^{-1}. These 12 conformers have mutual backbone RMS deviation of 0.90 ± 0.22 Å, and all of the residues are distributed in the most favored or the additional allowed regions. Then, a Gaussian distribution function was used to assign a probability ω_{ij}, averaged over all 12 conformers, for a given disulfide bridge to occur in each of them on the basis of the corresponding intercystinyl $C^{\beta i}-C^{\beta j}$ distance or $S^{\gamma i}-S^{\gamma j}$ distance. Subsequently, the probability $\Pi(\omega_{ij})$ for each of disulfide bridge pattern to occur within each of the 12 conformers was obtained by multiplying the averaged probabilities ω_{ij} of the five individual disulfide bridges of the pattern. All these analyses were performed by a self-compiled program of C language.

Structure Calculations. The experimental constraints include interproton distance restraints, dihedral angle restraints, and hydrogen bond restraints. Interproton distance restraints were derived from cross-peaks in the NOESY spectra, which were calibrated by the peak intensities with known distances (1.79 Å for the distance between two hydrogen of methylene) (*18*). The NOEs were classified based on peak intensities as strong, medium, weak, and very weak, corresponding to distance restraints with an upper limit of 2.7, 3.5, 5.0, and 6.0 Å, respectively. Pseudoatom corrections were applied to the upper limits of degenerate of unassigned methylene, methyl, and aromatic ring groups (*18*). The dihedral ϕ angle restraints were obtained by the $^3J_{HN-H\alpha}$ coupling constants measured from either 1D NMR spectra or the antiphase cross-peak splitting in a high-digital resolution DQF-COSY.

Structural calculations were performed using standard simulated annealing (SA) protocols implemented in the CNS solve 1.1 (*17*) starting from an extended polypeptide chain. The procedure include a constant high-temperature torsion angle annealing protocol (*14*), a slow cooling stage with torsion angle dynamics, an Cartesian dynamics cooling stage, and 2000 steps of energy minimization. The final values used for the scale factors were 75 kcal mol^{-1} Å^{-2} for experimental distance restraints, 200 kcal mol^{-1} Å^{-2} for dihedral restraints, and 1.0 kcal mol^{-1} Å^{-2} for the van der Waals repulsion term. The calculated structures were analyzed with AQUA and PROCHECK-NMR programs (*19*) and MOLMOL program (*20*).

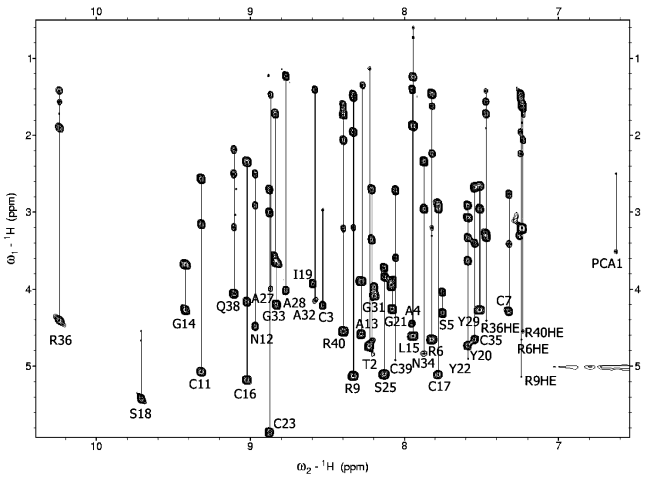

FIGURE 2: The α-N region of TOCSY spectrum (with mixing time of 80 ms) of EAFP2 in H_2O at pH 5.6 and temperature of 290 K, showing the intraresidue scalar connectivities.

RESULTS

NMR Data, Resonance Assignment, and Secondary Structure. EAFP2 was purified from the bark of *E. ulmoides* Oliv as described previously (*11*). This peptide yielded NMR spectra with good chemical shift dispersion in the amide region (Figure 2), providing a good indication of well-defined structure. Some other spectra including the part of α−α region of the NOESY spectrum shown in Supporting Information demonstrate the good quality of the data. Sequence-specific assignment of the ^{1}H NMR resonance of EAFP2 was performed by using the well-established sequence assignment strategy proposed by Wüthrich (*18*). Despite the good dispersion of amide proton chemical shifts, some peak overlaps could be detected in the spectra at temperature of 300 K, which can be unambiguously resolved in the spectra at 290 K (Arg9 and Arg40) or in solution of ^2H_2O (Gly26, Cys30, and Cys37; Leu15 and Ala4; Tyr20 and Tyr22) (data not shown).

All residues of EAFP2 could be sequentially assigned either via $d_{\alpha N}$ and/or d_{NN} NOEs, with the exception of Cys37−Glu38 that was sequentially assigned via $d_{\beta N}$ NOEs, Cys7−Pro8 via $d_{\alpha\alpha}$ NOEs, Pro8−Arg9 via $d_{\delta N}$ NOEs and Arg9−Pro10 via $d_{\alpha\delta}$ NOEs, as shown in Figure 3A. The $d_{\alpha\alpha}$ NOEs of Cys7−Pro8 indicated the cis-peptide bond between Cys7 and Pro8 (Figure 3A).

The delineation of the regular secondary structure of EAFP2 from NMR data is based on the characteristic set of interstrand αH_i-NH_j, NH_i-αH_j, and αH_i-αH_j NOE cross-peaks, $^3J_{HN-H\alpha}$ coupling constants, and slowly exchanging amide protons (shown in Figure 3A,B). The strong NOE cross-peaks of NH_i-NH_{i+1} and medium NOE cross-peaks of αH_i-NH_{i+1}, αH_i-NH_{i+2}, αH_i-NH_{i+3}, and αH_i-NH_{i+4} between Gly26−Cys30 (Figure 3A) suggest the existence of a short α-helix. A similar NOE pattern with lack of αH_i-NH_{i+4} cross-peak is found between Cys3−Arg6 (Figure 3A), which

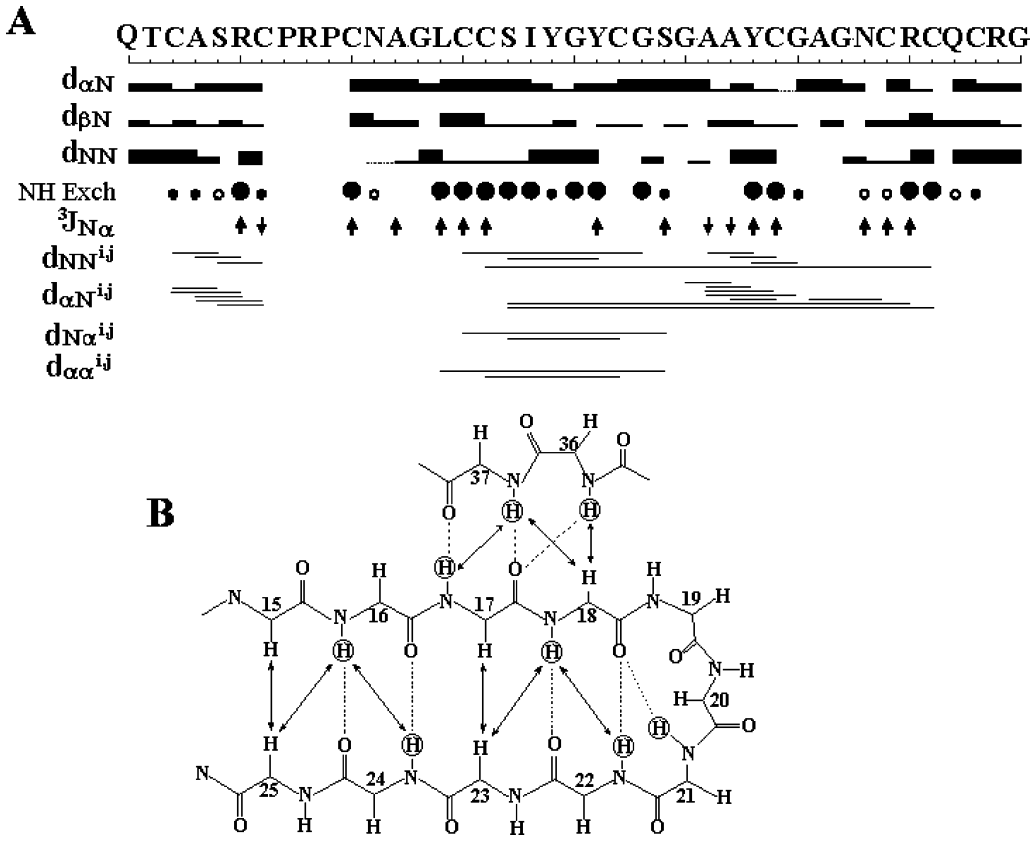

FIGURE 3: (A) Overview of the structural data for EAFP2 obtained from the NMR data. Sequential NOEs from the spectra with mixing time of 100 or 200 ms are categorized in distance ranges $d < 2.7$ Å (thick bars), $2.7 \leq d \leq 3.5$ Å (thin bars), $d > 3.5$ Å (lines) Å; the dotted lines show the NOEs only in the spectra with mixing time of 400 ms; the amide $^1H/^2H$ exchange rates after 48 h (large solid circles), 24 h (small solid circles), and 4 h (small empty circles); and the coupling constants $^3J_{N\alpha} > 8.5$ Hz (up arrows), < 5.5 Hz (down arrows). (B) Schematic representation of the antiparallel β-sheet structure of EAFP2 deduced from analysis of the NMR data. The arrowed lines indicate the observed interstrand NOE connectivities. The dotted lines show the hydrogen bonds derived from the NOE patterns and slowly exchanging amide protons as well as the preliminary NOE-based structure. The observed slowly exchanging amide protons in the β-sheet are circled.

indicates a possible 3_{10} helical turn between Cys3−Arg6. In addition, EAFP2 appears to comprise a three-strand antiparallel β-sheet (β1, β2, β3 corresponding to residues 16−18, 22−24, 36−37, respectively). These secondary structural elements were further validated by slowly exchanging amide protons and a hydrogen-bonding system from the tertiary structure calculation.

Assignment of the Disulfide Bridges. EAFP2 contains 10 cysteines that form five pairs of disulfide bridges. These 10 cysteines can potentially form 45 different disulfide bridges that can be arranged into 945 kinds of possible disulfide patterns calculated by the method described by Klaus et al (*16*). The statistic results show the disulfide pattern (1−5, 2−9, 3−6, 4−7, 8−10) displayed the obvious probability, irrespective of the choice of the atom (Cβ or Sγ) and the dispersion parameter **s**. The results indicated that the disulfide-pairing pattern of EAFP2 is Cys3−Cys17, Cys7−Cys37, Cys11−Cys23, Cys16−Cys30, and Cys35−Cys39.

The proposed disulfide pairings are entirely compatible with our previously prediction (*11*). Four pairs of disulfide bonds (Cys3−Cys17, Cys11−Cys23, Cys16−Cys30, and Cys35−Cys39) correspond to the disulfide bridges in hevein and hevein domains found in plant chitin-binding proteins (*2, 9*−*10*). The additional pair of disulfide bond connects the N-terminal Cys7 and the C-terminal Cys37 of EAFP2.

Structure Calculation and Refinement. In the first stage of structure calculation, only dihedral angle restraints and NOE distance restraints that assigned unambiguously were used. Then, the hydrogen-bonding pattern was included as restraints for regular secondary structural elements since their existence was detected in the preliminary, NOE-based structures and can be unambiguously corroborated by slow $^1H/^2H$ exchange data and the analysis of the NOE pattern (Figure 3) (*18*). In the final cycle of the calculation, the above-proposed disulfide bonds were included as S−S covalent bonds and all the experimental restraints included 20 hydrogen bond restraints, 16 dihedral angle restraints, and 594 distance restraints were used. The N-terminus was patched into the pyroglutamic group according to the parameters of molecule LPYGLU in the Cambridge Structural Database (CSD). The restraints used in the calculation of the EAFP2 structure are summarized in Table 1.

A total of 100 structures were calculated, in which 97 structures were accepted with no distance violation larger than 0.2 Å, no dihedral violation larger than 2 degrees, and the total energy less than 20 kcal mol^{-1}. From these 97 structures, the 20 convergent structures were selected with lowest energy, best structural quality in Ramachandran plot, and lowest mutual RMS deviation. The 20 structures have been analyzed using AQUA and PROCHECK-NMR (*19*). The statistical data for these 20 structures are presented in Table 1. The distribution in the Ramachandran plot of all the residues indicates the overall quality: 73.2% of the residues are in the most favorable region and 26.8% in the general region. The 20 structures have neither violations of NOE greater than 0.1 Å, nor of dihedral angles larger than 2.0 degrees. The backbone of the 20 structures could be defined with an RMS deviation value of 0.65 (±0.13) Å for residues 3−39 and 1.28 (±0.20) Å for heavy atom.

Description of the Structure. The set of 20 conformers representing the solution structure of EAFP2 is shown in Figure 4A. EAFP2 adopts a compact globular fold comprising a 3_{10} helix (Cys3−Arg6), an antiparallel β-sheet composed by three beta-strands (β1, β2, and β3; Cys16−Ser18, Tyr22−Gly24, and Arg36−Cys37), and an α-helix (Gly26−Cys30) (Figure 4B). The antiparallel β-sheet acts as the core of the protein which is mainly stabilized by hydrogen bonds between the strands, in which there are six hydrogen bonds including NH16−O24, NH17−O37, NH18−O22, NH22−O18, NH24−O16, and NH37−O17. The existence of these hydrogen bonds is supported by a slow $^1H/^2H$ exchange rate for amide protons of residues 16, 17, 18, 22, 24, and 37 (Figure 3A, B). The rest of the protein more or less covers the core β-sheet structure. Four hydrogen bonds NH6−O3, NH7−O4, NH29−O25, and NH30−O26 exist in the α-helix and 3_{10} helix, which are also evidenced by the slow $^1H/^2H$ exchange for residues 6, 7, 29, and 30 (Figure 3A).

Six regular β-turns are identified in the connecting segments according to the notation of Hutchinson (*22*) with center around Cys7 and Pro8, Pro8 and Arg9, Ala13 and Gly14, Ile19 and Tyr20, Ala32 and Gly33, and Cys39 and Arg40, respectively. It is worth noting that *turn*1 and *turn*2 form nested *β-turn*s of *ViaI*-type and *VIII*-type, respectively.

The tertiary structure of EAFP2 has a significant character in residue distribution. The five hydrophobic and aromatic residues (Leu15, Ile19, Tyr20, Tyr22, and Tyr29) are distributed on one side of the tertiary structure, and the four cationic residues (Arg6, Arg9, Arg36, and Arg40) are concentrated on its opposite side (Figure 4C) though these cationic residues are located in the N-terminal and C-terminal part in the amino acid sequence of the peptide. All these

Table 1: NMR-Derived Restraints and the Structural Statistics for the 20 Final Lowest Energy Structures of EAFP2

A. NMR-Derived Restraints	
total no. of distance restraints	614
intraresidue	182
sequential ($i - j = 1$)	164
short range ($1 < i - j < 5$)	89
long range ($i - j > 4$)	159
hydrogen bond	20
dihedral restraints (ϕ)	16
total restraints per residue	15.4
B. Structural Quality	
no. of restraint violation	
distance (>0.1 Å)	0
dihedral (>2 degree)	0
energetic statistics (kcal/mol)	
E_{total}	13.87 ± 1.90
E_{bonds}	0.74 ± 0.17
E_{angle}	8.33 ± 0.87
E_{impro}	0.44 ± 0.06
E_{vdw}	3.95 ± 0.99
RMSD from experimental restraints	
NOE distance restraints (Å)	0.0029 ± 0.0005
dihedral angle restraints (deg.)	0.0343 ± 0.0205
RMSD from idealized geometry	
bonds (Å)	0.0012 ± 0.00013
angles (deg)	0.2382 ± 0.0122
impropers (deg)	0.0994 ± 0.0063
Ramachandran analysis	
most favored regions (%)	73.2
additionally allowed regions (%)	26.8
generously allowed regions (%)	0.0
disallowed regions (%)	0.0
C. Coordinate Precision (Å, mean/pairwise)	
RMSD (Å) of residue 3−39	
backbone atoms	0.65 ± 0.13
heavy atoms	1.28 ± 0.20

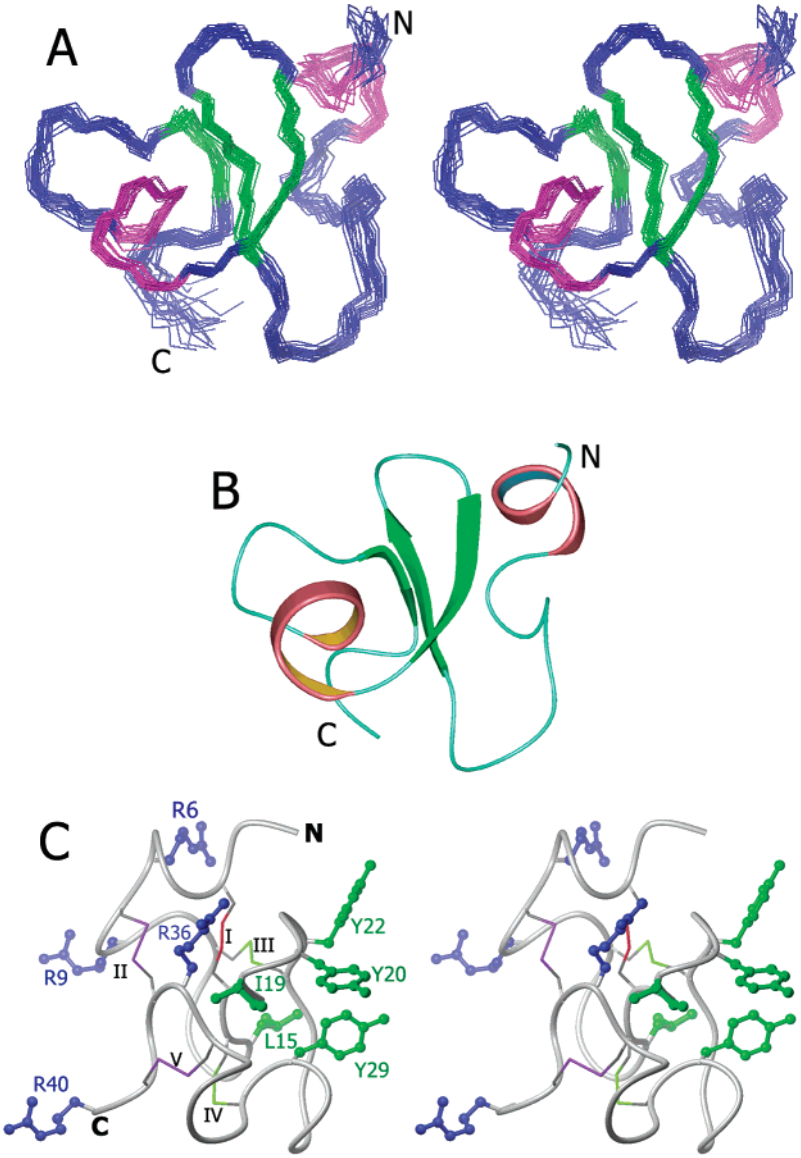

FIGURE 4: The NMR structure diagrams of EAFP2. (A) Stereo plot of the 20 best three-dimensional structures of EAFP2 (under PDB accession code: 1P9Z) superimposed with their energy-minimized average structure over the backbone of well-defined residues 3−39. Green represents the β-sheet and magenta the helix. (B) The backbone ribbon diagram of representative model structure 1 of EAFP2 in orientation as (A), showing helix (in orange) and β-sheet (in green). (C) The stick drawing of EAFP2 showing the disulfide bonds as well as the hydrophobic and hydrophilic side chains. The five pairs of disulfide bridges are indicated by I, II, III, IV, and V corresponding to Cys3−Cys17, Cys7−Cys37, Cys11−Cys23, Cys16−Cys30, and Cys35−Cys39, respectively. The four positive charged residues (Arg6, Arg9, Arg36, and Arg40) are in blue, and the five hydrophobic residues (Leu15, Ile19, Tyr20, Tyr22, and Tyr29) are in green. The diagrams are prepared by MOLMOL program (*20*).

residues are exposed on the surface of the molecule so as to form a hydrophobic face and a cationic face, respectively, which are roughly opposite each other (Figure 4C). Because of the characteristic residue distribution, EAFP2 displays a significant amphiphilic character (Figure 5B). This is the most striking feature of the EAFP2 structure.

This amphipathic character in the tertiary arrangement of the residues is closely related to the distinct five-disulfide pairing pattern of EAFP2. On the basis of inspecting the location of disulfide bonds in the structure, the bridges Cys11−Cys23 and Cys16−Cys30 (III and IV in Figure 4C) connect the middle segment from Cys11 to Cys30, which contains all of the five hydrophobic residues (Leu15, Ile19, Tyr20, Tyr22, and Tyr29) that form the hydrophobic face. Thus, these two disulfide bridges are the main structure elements to stabilize the hydrophobic face. The disulfide bond Cys35−Cys39 (V in Figure 4C) stabilizes the C-terminal local conformation and restrains the location of two cationic residues (Arg36 and Arg40) at this area. The unique disulfide bond Cys7−Cys37 (II in Figure 4C) draws the N-terminal segment close to the C-terminal part and, in turn, brings two positively charged residues Arg6 and Arg9 together with Arg36 and Arg40 to form the cationic face (Figure 4C). Evidently, the disulfide bond Cys7−Cys37 distinct from chitin-binding peptides mainly contributes to the formation of the cationic face of EAFP2. In fact, the significant structure difference between EAFP2 and hevein is just at the part related to this disulfide bond. Besides, the disulfide bond Cys3−Cys17 (I in Figure 4C) seems to play the role of a link between two parts of the structure described above.

The three-dimensional structure of EAFP2 showed that the addition of the fifth unique disulfide bond Cys7−Cys37

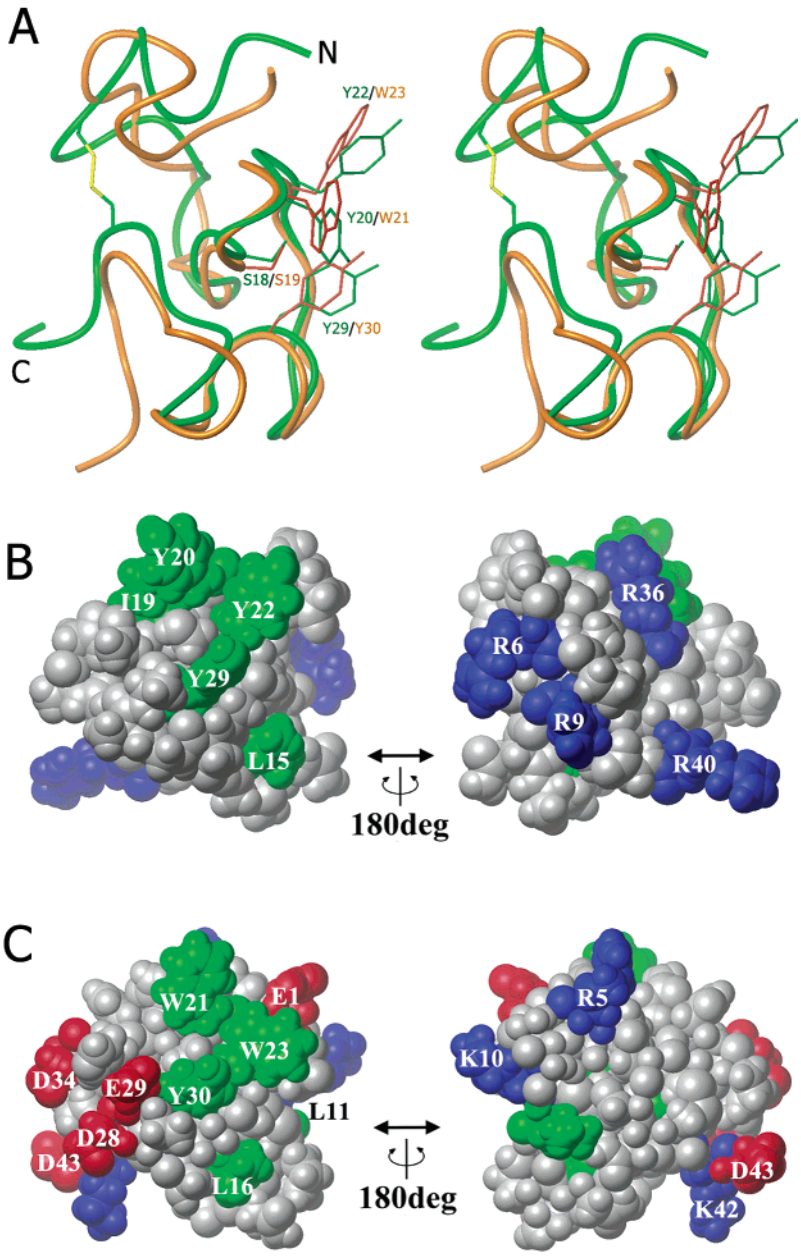

FIGURE 5: The structure comparison between EAFP2 and hevein (PDB code: 1hev). (A) The ribbon drawing of EAFP2 (in green) superimposed with hevein (in orange) by α-carbon atoms of residues 11−30 of EAFP2 with corresponding atoms of residues 12−31 of hevein. The sticks show the side chains of the aromatic residues and one serine that are directly involved in protein−carbohydrate binding (chitin-binding site) and the distinct disulfide bond Cys7−Cys37 of EAFP2 in yellow. (B) Space-filling drawing of EAFP2, showing the well-defined amphipathic surface. (C) Space-filling drawing of hevein, which lacks the amphipathic topology. The orientations of (B) and (C) are like that of (A) turned 90° left or right about the vertical axis. The positively and negatively changed residues and the hydrophobic residues are shown in blue, red, and green, respectively. Drawings were prepared by using MOLMOL program (*20*).

gives rise to the tertiary structural character to EAFP2, which should be related to the functional property of EAFP2, i.e., affecting both chitin-containing and chitin-free fungi.

DISCUSSION

EAFP2 is distinct with a five-disulfide motif and dual antifungal activities against both chitin-containing and chitin-free fungi, although it has the same critical residues of the chitin-binding domain as in hevein and hevein-like peptide shown in Figure 1. The NMR structure of EAFP2 revealed that the additional unique disulfide bridge (Cys7−Cys37, II in Figure 4C) induced the new structural feature in this type of peptide, which should be the main structural basis of the peculiar functional properties of EAFP2.

Structure Comparison with Hevein. Hevein is a representative member of the hevein-like peptide. The NMR structures of hevein and hevein-chitobiose complex revealed a chitin-binding domain in the molecular scaffold and the tertiary arrangement of the chitin-binding site (*5*, *23*). The hevein domain has also been found in a variety of plant chitin-binding proteins such as wheat germ agglutinin (WGA) (*24*−*26*) and nettle lectin (UDA) (*27*−*28*). The X-ray crystal structures of WGA and UDA showed four and two consecutive hevein domains in these molecules, respectively.

The structure comparison between EAFP2 and hevein shows that the region from residue Cys11 to Cys30 in EAFP2 can be well superimposed with the corresponding segment of hevein, which has a good fit by an α-carbon deviation of

1.143 Å for the averaged structures (Figure 5A). This part is just the core of the chitin-binding domain of hevein and corresponds to the hydrophobic face of EAFP2 described above, which is cross-linked by disulfide bridges Cys11−Cys23 and Cys16−Cys30. Evidently, EAFP2 possesses the chitin-binding domain similar to that in hevein.

The significant structural differences between EAFP2 and hevein appeared at the N-terminal 10 residues and the C-terminal segment (Figure 5A). In hevein, these two parts are rather free and far from each other because there is no any tertiary restraint in between. In EAFP2, the unique disulfide bond Cys7−Cys37 cross-links these two parts to form a distinct sector that features a cationic face as described previously (Figure 5A). The C-terminal tail of EAFP2 forms a β-turn centered on residues 39−40, which makes the orientation of the C-terminus much different from that of hevein and restrains the residue Arg40 on the molecular surface. The disulfide bridge Cys7−Cys37 distinctly appearing in EAFP2 brings the neighboring residues Arg6 and Arg9 onto the surface of this sector in association with Arg36 and Arg40 to form the cationic face. In the N-terminal segment of EAFP2, residues Arg6−Pro10 adopts a dramatically different conformation with a distinct nested β-turns of *ViaI*-type and *VIII*-type, in which Pro8 has a cis conformation. This special local structure may be favorable to the side chain of Cys7 in proper orientation to form the bridge with Cys37.

Evidently, compared with hevein, the most striking feature of EAFP2 is a new structural sector formed by N-terminal and C-terminal residues through cross-linking of a unique disulfide bond Cys7−Cys37, which gives EAFP a more well-defined amphipathic character (Figure 5B). In comparison, hevein does not have the cationic face and lacks the amphipathic topology as shown in Figure 5C. Such structural difference may underlie the unique antifungal properties of EAFP.

In addition, despite these structural changes, the N-terminal pyroglutamate residue of EAFP2 is still regulated to be adjacent to the aromatic ring of Tyr22, which can be also evidenced by a series of significant NOE cross-peaks between these two residues (data not shown). The similar relationship can be found in the structures of hevein, Ac-AMP and the A domain of UDA, which implies that the N-terminal residue should play a role in maintaining the side chain orientation of Tyr22 critical in binding with chitin.

The Chitin-Binding Site of EAFP2. Polysaccharide binding assay showed that EAFP2, like hevein and Ac-AMP, can bind with crab shell chitin specifically (*11*). For hevein and Ac-AMP, segments of residues Cys12 to Cys31 and Cys9 to Cys28 were identified as an essential chitin-binding domain, respectively (*7*, *23*). This structural motif has also been found in several other plant chitin-binding proteins mentioned above (*24*−*28*). The aromatic side chain groups of Trp21, Trp23, and Trp30 of hevein are known to bind specifically to chitin-derived oligosaccharides through hydrophobic interactions (*29*, *30*). This binding is further strengthened by hydrogen bonding with Ser19 of hevein (*30*). These three aromatic residues and one serine are also conserved in other hevein-like peptide and hevein domains of plant chitin-binding proteins such as WGA (*24*−*26*) and UDA (*27*−*28*).

As shown in Figure 5A, the structure of residues Cys11−Cys30 of EAFP2 is well superimposed with the corresponding segments of hevein. The residues of Ser18, Tyr20, Tyr22, and Tyr29 of EAFP2 are located at perfectly corresponding positions to those residues critical for chitin binding in hevein (Ser19, Trp21, Trp23, and Tyr30). Therefore, one could reasonably assume that EAFP2 possesses a chitin-binding site consisting of residues Ser18, Tyr20, Tyr22, and Tyr29 (Figure 5A), which may interact with chitin by the same mechanism as observed in hevein (*29*−*30*).

The Structural Basis for the Activity of Inhibiting the Chitin-Free Fungi. In addition to the chitin-binding domain, all four positively charged residues of EAFP2, Arg6, Arg9, Arg36, and Arg40 from the N- and C-terminal segments are distributed on the same side of the exterior surface to form a cationic face that is stabilized by disulfide bridges Cys7−Cys37 and Cys35−Cys39 (II and V in Figure 4C). On the basis of the knowledge on antimicrobial peptides known so far, this cationic face may play a critical role in inhibiting the growth of the cell wall chitin-free fungus (*31*). In the past decade, a variety of antimicrobial peptides have been discovered, which showed diverse structures from the amphiphilic helical structure, β-sheet structure to the helix-β-sheet motif, etc (*1*, *31*, *32*). Despite the variety of the structures most of these antifungal peptides have an amphiphilic surface in which clusters of hydrophobic and cationic residues are spatially organized in discrete sectors of the molecule ("amphipathic" design) (*1*, *31*). The synthetic analysis suggests that the cationic sector may be critical for the antimicrobial activity through binding to the negatively charged phospholipid of the microbial cell membrane (*31*). Such interactions could play a role in the initial binding of antimicrobial peptides with cell membrane to disturb the normal membrane functions and even the pore formation in the cell membrane together with molecular amphipathic design (*1*, *31*). EAFP2 may take the same approach to affect on the cell wall chitin-free fungus. Besides the bioassay showed that the antifungal effects of EAFP2 could be strongly antagonized by calcium ion (*11*), which identified that the inhibiting activities of EAFP2 certainly depend on the electrostatic interaction. Most probably the hydrophobic face (Figure 4C and 5B) containing the chitin-binding site of EAFP2 also contributes to the performance of the inhibiting activities on the chitin-free fungi with nonspecific hydrophobic interactions. On the basis of the structural feature of EAFP2, it can be reasonably assumed that EAFP2 may have antibacterial activities, although no experimental data currently exists.

In summary, as a novel antifungal peptide distinct with a five-disulfide motif and effects on both chitin-containing and chitin-free fungi, EAFP2 has a tertiary structure containing a chitin-binding domain (residues 11−30) with a hydrophobic face and a characteristic sector formed by the N-terminal 10 residues and the C-terminal segment cross-linked by the unique disulfide bridge Cys7−Cys37, which brings all four positively charged residues (Arg6, Arg9, Arg36, and Arg40) onto a cationic face. On the basis of such a structure feature, EAFP2 may take two kinds of antifungal mechanisms. One is dependent on the chitin-binding activity for the chitin-containing fungi, while another is through the amphiphilic surface, especially the cationic face to interact with the fungal membrane. In association with the distinct five disulfide

motif, EAFP2 may be considered as a new type of the antifungal peptide.

SUPPORTING INFORMATION AVAILABLE

Included are the proton chemical shifts in H_2O solution, the alpha-N regions of DQF-COSY, TOCSY, and NOESY spectra and a part of alpha−alpha region of NOESY spectrum as well as the Ramachandran plot of 20 energy-minimized structures of EAFP2. This material is available free of charge via the Internet at http://pubs.acs.org.

REFERENCES

1. Zasloff, M. (2002) Antimicrobial peptides of multicellular organisms. *Nature 415*, 389−395.
2. Broekaert, W. F., Cammue, B. P. A., De Bolle, M. F. C., Thevissen, K,, De Samblanx, G. W., and Osborn, R. W. (1997) Antimicrobial peptides from plants. *Crit. Rev. Plant Sci. 16*, 297−323.
3. Garcia-Olmedo, F., Molina, A., Alamillo, J. M., and Rodriguez-Palenzuela, P. (1998) Plant defense peptides. *Biopolymers 47*, 479−491.
4. Broekaert, I., Lee, H. I., Kush, A., Chua, N. H., and Raikhel, N. (1990) Wound-induced accumulation of mRNA containing a hevein sequence in laticifers of rubber tree (*Hevea brasiliensis*). *Proc. Natl. Acad. Sci. U.S.A. 87*, 7633−7637.
5. Andersen, N. H., Cao, B., Rodriguez-Romero, A., and Arreguin, B. (1993) Hevein: NMR assignment and assessment of solution-state folding for the agglutinin-toxin motif. *Biochemistry 32*, 1407−1422.
6. Broekaert, W. F., Marien, W., Terras, F. R., De, Bolle, M. F., Proost, P., Van Damme, J., Dillen, L., Claeys, M., Rees, S. B., Vanderleyden, J., and Commue, B. P. A. (1992) Antimicrobial peptides from *Amaranthus caudatus* seeds with sequence homology to the cysteine/glycine-rich domain of chitin-binding proteins. *Biochemistry 31*, 4308−4314.
7. Martins, J. C., Maes, D., Loris, R., Pepermans, H. A., Wyns, L., Willem, R., and Verheyden, P. (1996) NMR study of the solution structure of Ac-AMP2, a sugar binding antimicrobial protein isolated from Amaranthus caudatus. *J. Mol. Biol. 258*, 322−333.
8. Koo, J. C., Lee, S. Y., Chun, H. J., Cheong, Y. H., Choi, J. S., Kawabata, S., Miyagi, M., Tsunasawa, S., Ha, K. S., Bae, D. W., Han, C. D., Lee, B. L., and Cho, M. J. (1998) Two hevein homologs isolated from the seed of *Pharbitis nil* L. exhibit potent antifungal activity. *Biochim. Biophys. Acta 1382*, 80−90.
9. Raikhel, N. V., and Lee, H. I. (1993) Structure and function of chitin-binding proteins. *Plant Mol. Biol. 44*, 591−615.
10. Broekaert, W. F., Parijs, J. V., Leyns, F., Joos, H., and Peumans, W. J. (1989) A chitin-binding lectin from stinging nettle rhizomes with antifungal properties. *Science 245*, 1100−1102.
11. Huang, R. H., Xiang, Y., Liu, X. Z., Zhang, Y., Hu, Z., and Wang, D. C. (2002) Two novel antifungal peptides distinct with a five-disulfide motif from the bark of *Eucommia ulmoides* Oliv. *FEBS Lett. 521*, 87−90.
12. Huang, R. H., Zhang, Y., and Wang, D. C. (2003) Primary structural determination of N-terminally blocked peptides from the bark of *Eucommia ulmoides* Oliv by mass spectrometric analysis. *Rapid Commun. Mass Spectrom. 17*, 903−908.
13. Liu, X. Z., Hu, Z., Li, Y., Yang, J. B., and Li, B. J. (1994) Isolation and characterization of an antifungal protein from the bark of *Eucommia ulmoides*. *Acta Bot. Yunnanica 16*, 385−391.
14. Stein, E. G., Rice, L. M., and Brunger, A. T. (1997) Torsion-angle molecular dynamics as a new efficient tool for NMR structure calculation. *J. Magn. Reson. 124*, 154−164.
15. Goddard, T. D., and Kneller, D. G. (2001) *SPARKY 3*, University of California, San Francisco.
16. Klaus, W., Broger, C., Gerber, P., and Senn, H. (1993) Determination of the disulphide bonding pattern in proteins by local and global analysis of nuclear magnetic resonance data. *J. Mol. Bi*ol. *232*, 897−906.
17. Wüthrich, K. (1986) *NMR of Proteins and Nucleic Acids*, John Wiley, New York.
18. Brünger, A. T., Adams, P. D., Clore, G. M., DeLano, W. L., Gros, P., Grosse-Kunstleve, R. W., Jiang, J. S., Kuszewski, J., Nilges, M., Pannu, N. S., Read, R. J., Rice, L. M., Simonson, T., and Warren, G. L. (1998) Crystallography & NMR system: A new software suite for macromolecular structure determination. *Acta Crystallogr., Sect. D: Biol. Crystallogr. 54*, 905−921.
19. Laskowski, R. A., Rullmannn, J. A., MacArthur, M. W., Kaptein, R., and Thornton, J. M. (1996) AQUA and PROCHECK-NMR: programs for checking the quality of protein structures solved by NMR. *J. Biomol. NMR 8*, 477−486.
20. Koradi, R., Billeter, M., and Wuthrich, K. (1996) MOLMOL: A program for display and analysis of macromolecular structures. *J. Mol. Graphics 14*, 51−55, 29−32.
21. Gao, G. H., Liu, W., Dai, J. X., Wang, J. F., Hu, Z., Zhang, Y., and Wang, D. C. (2001) Solution structure of PAFP−S: A new knottin-type antifungal peptide from the seeds of *Phytolacca Americana*. *Biochemistry 40*, 10973−10978.
22. Hutchinson, E. G., and Thornton, J. M. (1994) A revised set of potentials for beta-turn formation in proteins. *Protein Sci. 3*, 2207−2216.
23. Asensio, M. L., Canada, F. J., Bruix, M., Rodriguez-Romero, A., and Jimenez-Barbero, J. (1995) The interaction of hevein with *N*-acetylglucosamine-containing oligosaccharides. Solution structure of hevein conplexed to chitobiase. *Eur. J. Biochem. 230*, 621−633.
24. Wright, C. S. (1990) 2.2 Å resolution structure analysis of two refined *N*-acetylneuraminyl-lactose-wheat germ agglutinin isolectin complexes. *J. Mol. Biol. 215*, 635−651.
25. Wright, C. S. (1992) Crystal structure of a wheat germ agglutinin/glycophorin- sialoglycopeptide receptor complex. Structural basis for cooperative lectin-cell binding. *J. Biol. Chem. 267*, 14345−14352.
26. Wright, C. S., and Jaeger, J. (1993) Crystallographic refinement and structure analysis of the complex of wheat germ agglutinin with a bivalent sialoglycopeptide from glycophorin A. *J. Mol. Biol. 232*, 620−638.
27. Harata, K., and Muraki, M. (2000) Crystal structures of *Urtica dioica* agglutinin and its complex with tri-*N*-acetylchitotriose. *J. Mol. Biol. 297*, 673−681.
28. Saul, F. A., Rovira, P., Boulot, G., Damme, E. J., Peumans, W. J., Truffa-Bachi, P., and Bentley, G. A. (2000) Crystal structure of Urtica dioica agglutinin, a superantigen presented by MHC molecules of class I and class II. *Struct. Folding Des. 8*, 593−603.
29. Asensio J. L., Canada F. J., Bruix M., Gonzalez C., Khiar, N., Rodriguez-Romero A., and Jimenez-Barbero, J. (1998) NMR investigations of protein-carbohydrate interactions: refined three-dimensional structure of the complex between hevein and methyl beta-chitobioside. *Glycobiology 8*, 569−577.
30. Asensio, J. L., Canada, F. J., Siebert, H. C., Laynez, J., Poveda, A., Nieto, P. M., Soedjanaamadja, U. M., Gabius, H. J., and Jimenez-Barbero, J. (2000) Structural basis for chitin recognition by defense proteins: GlcNAc residues are bound in a multivalent fashion by extended binding sites in hevein domains. *Chem. Biol. 7*, 529−543.
31. Hwang, P. M., and Vogel, H. J. (1998) Structure−function relationships of antimicrobial peptides. *Biochem. Cell. Biol. 76*, 235−246.
32. Aumelas, A., Mangoni, M., Roumestand, C., Chiche, L., Despaux, E., Grassy, G., Calas, B., and Chavanieu, A. (1996) Synthesis and solution structure of the antimicrobial peptide protegrin-1. *Eur. J. Biochem. 237*, 575−583.

BI036263Y